ANTIOXIDANTS & REDOX SIGNALING
Volume 15, Number 8, 2011

DOI: 10.1089/ars.2010.3341

High-Mobility Group Box 1 Release and Redox Regulation Accompany Regeneration and Remodeling of Skeletal Muscle

Michela Vezzoli,[1] Patrizia Castellani,[2] Gianfranca Corna,[1] Alessandra Castiglioni,[1] Lidia Bosurgi,[3] Antonella Monno,[3] Silvia Brunelli,[4] Angelo A. Manfredi,[3] Anna Rubartelli,[2,*] and Patrizia Rovere-Querini[1,*]

Abstract

High-mobility group box 1 (HMGB1), a damage-associated molecular pattern (DAMP) molecules, favors tissue regeneration *via* recruitment and activation of leukocytes and stem cells. Here we demonstrate, in a model of acute sterile muscle injury, that regeneration is accompanied by active reactive oxygen species (ROS) production counterbalanced and overcome by the generation of antioxidant moieties. Mitochondria are initially responsible for ROS formation. However, they undergo rapid disruption with almost complete disappearance. Twenty-four hours after injury, we observed a strong induction of MURF1 and atrogin-1 ubiquitin ligases, key signals in activation of the proteasome system and induction of muscle atrophy. At later time points, ROS generation is maintained by nonmitochondrial sources. The antioxidant response occurs in both regenerating fibers and leukocytes that express high levels of free thiols and antioxidant enzymes, such as superoxide dismutase 1 (SOD1) and thioredoxin. HMGB1, a protein thiol, weakly expressed in healthy muscles, increases during regeneration in parallel with the antioxidant response in both fibers and leukocytes. A reduced environment may be important to maintain HMGB1 bioactivity. Indeed, oxidation abrogates both muscle stem cell migration in response to HMGB1 and their ability to differentiate into myofibers *in vitro*. We propose that the early antioxidant response in regenerating muscle limits HMGB1 oxidation, thus allowing successful muscle regeneration. *Antioxid. Redox Signal*. 15, 2161–2174.

Introduction

> "***Scintilla**, che gran **fiamma** seconda"*
> *A mighty flame followeth a tiny spark.*
> —*Dante Alighieri*

SIGNALS PRODUCED BY MICROBES, referred to as pathogen-associated molecular patterns, initiate the inflammatory response during infection, *via* the activation of dedicated pattern recognition receptors on leukocytes. Inflammation also initiates in response to threats to tissue and organ integrity, even in the absence of invading pathogens. Tissue repair is an outcome of both responses, aimed at restoring tissue homeostasis. Endogenous damage-associated molecular patterns (DAMPS), also referred to as alarmins, are key signals of necrosis (4, 32, 38, 48, 65). DAMPs are involved in the early recruitment of inflammatory cells and in their local activation and differentiation, so that they can instruct local stem and progenitor cells.

The high-mobility group box 1 (HMGB1) protein, originally identified for its nuclear role, is also now one of the best-characterized DAMPs, playing a nonredundant role in sepsis (64). HMGB1 has an inflammatory function, behaving at the site of tissue injury as a potent attractor for inflammatory leukocytes, such as neutrophils and monocytes (39, 47). It also serves as a chemotactic factor for stem cells, including endothelial precursor cells (12) and vessel-associated mesoangioblasts (41, 42). HMGB1 actively favors regeneration in models of cutaneous wound healing and of myocardial and peripheral tissues ischemia [see *e.g.* (5, 16, 19, 27, 28, 54)] and activates VEGF-dependent angiogenesis in models of diabetes mellitus (5).

[1]Innate Immunity and Tissue Remodeling Unit, San Raffaele Scientific Institute, Milano, Italy.
[2]Cell Biology Unit, National Cancer Research Institute, Genova, Italy.
[3]Autoimmunity & Vascular Inflammation Unit, San Raffaele Scientific Institute, Vita-Salute San Raffaele University, Milano, Italy.
[4]Department of Experimental Medicine, Milano-Bicocca University, Milano, Italy.
*These two authors contributed equally to this work.

Most nucleated cells dying acutely by primary or post-apoptotic necrosis release HMGB1 (3, 51), either alone or as a multi-molecular complex associated with nucleosomes (60). Moreover, activated immune cells translocate HMGB1 from the nucleus to the cytoplasm and actively release it, thus re-creating in the surrounding environment signals associated with immunostimulatory, unscheduled necrotic cell death (6, 17, 18, 33, 34). Interestingly, HMGB1 has also recently been proposed as an endogenous regulator of autophagy (55, 56).

Systemic levels of HMGB1 may lead to shock and death (64). Thus, mechanisms that limit HMGB1 bioactivity should exist. HMGB1 is naturally bioactive in its reduced form (26, 61). The cysteine residues of HMGB1 are free and prevented from oxidation by the reducing conditions within the nucleus and cytosol. In contrast, the extracellular milieu is generally oxidizing, so in principle HMGB1 undergoes oxidation and consequent inactivation after its extracellular release. Oxidation may exert a key homeostatic function by limiting the biological activity of HMGB1 and other redox-sensitive moieties released by necrotic cells (57). The extracellular half-life of HMGB1 might be further shortened by the high levels of reactive oxygen species (ROS) released by eosinophils recruited within necrotic areas, a mechanism that has been proposed to limit chronic inflammation (31).

Increasing evidence suggests that the antioxidant response promotes extracellular effects and converts the extracellular environment to a more reduced state (9). How oxidizing (or reducing) the redox environment is outside cells during wound healing dictates how long extracellular HMGB1 remains bioactive and effectively able to recruit inflammatory cells. Reduced HMGB1, thus, activates stem and progenitor cells at the site of damage and influences the extent and the characteristics of tissue regeneration.

Skeletal muscle injury promotes early recruitment of cells of the innate immune system (polymorphonuclear leukocytes and monocytes/macrophages) and effective cross-talk between local and recruited cells, leading to the activation, proliferation, and fusion of satellite cells. These are muscle-specific stem cells located under the basal lamina of muscle fibers (1, 7, 59). Early after injury, inflammatory macrophages predominate and clear cellular debris. At later time points, macrophages acquire a phenotype associated with regeneration (7, 13, 14, 59). Innate cell activation in injured and regenerating muscles may also be deleterious. This is particularly so when damage persists, as occurs in the setting of muscular dystrophies.

Little is known about the redox changes triggered by muscle injury and their role in the regeneration process. These events are likely to influence multiple targets in each of the respective cell types. The molecular identification of elements within these pathways is critical for our understanding of skeletal muscle pathophysiology. The primary aim of this study was to determine whether HMGB1 was present at the site of injury and to dissect the role of redox in muscle regeneration and remodeling during the response to an acute sterile injury.

Materials and Methods

Acute muscle damage and evaluation of response to injury

Wild-type C57BL/6 female mice (from Charles River Laboratories) were injected intramuscularly with cardiotoxin (CTX, 50 μl, 50 μM within the quadriceps and 15 μM within the tibialis anterior [TA]) (*Naja mossambica mossambica*; Sigma-Aldrich). Mice were sacrificed at 1, 3, 7, 10, and 15 days after injury. Injured muscles were collected and frozen. Muscle damage, remodeling, and repair were evaluated by hematoxylin and eosin on 6-μm-thick muscle sections.

Staining procedures and confocal analyses

Serial cryostat sections from frozen muscles from mice before or at various times after injection with CTX were stained with the hydrogen peroxide (H_2O_2)-specific dye peroxy green (PG1) (obtained by C.J. Chan) and the sulphydryl-reactive dye Mercury Orange (Sigma-Aldrich) immediately after cutting as described (10, 62). Briefly, Mercury Orange was incubated 5 min on ice at a final concentration of 25 μM. To confirm the specificity of Mercury Orange binding to nonprotein thiols (NPSH, including glutathione [GSH] and cysteine), control sections were pretreated with 100 μM N-ethylmaleimide (Sigma-Aldrich) for 10 min to block thiol groups. Staining with PG1 (5 μM) was performed for 10 min at 37°C. To confirm the specificity of PG1 staining, control sections were pretreated with 1 mM dithiothreitol (DTT) for 10 min.

For mitochondria/ROS costaining, serial sections from the same muscle samples were fixed for 10 min in acetone, followed by incubation with MitoTracker (Molecular Probes), at 10 nM for 20 min. Sections were then washed with PBS and further incubated for 30 min with 10 mM 2′,7′-dichlorofluorescein diacetate (H_2DCFDA; Molecular Probes) followed by a rinse in PBS. The sections were analyzed by confocal microscopy, and the images were acquired by the Fluoview FV500 software (62).

Electron microscopy

TA muscle were dissected from mice and were fixed for 2 h at 4°C with 4% paraformaldehyde and 2.5% glutaraldehyde in 125 mM cacodylate buffer. Tissues were postfixed (1 h) with 2% OsO_4 in 125 mM cacodylate buffer, washed, and embedded in Epon. Conventional thin sections were collected on uncoated grids, stained with uranil and lead citrate, and examined with a Leo912 electron microscope.

RNA extraction and quantitative reverse transcriptase-polymerase chain reaction

Total cellular RNA was extracted from muscle using TRIZOL reagent (Applied Biosystems), following the manufacturer's recommendations. RNA (1 μg) was used for quantitative polymerase chain reaction (PCR) analysis for first-strand synthesis of complementary DNAs) with the high-capacity complementary DNA Reverse Transcription kit (Applied Biosystems) according to the manufacturer's instructions. Quantitative PCR was performed using SYBR-green PCR Master Mix (Applied Biosystems). The level of each RNA was normalized to the corresponding level of GAPDH messenger RNA (mRNA) for muscle lysates. Sequence of primers used in quantitative real-time PCR were as follows: Murf-1: 5′ ACCTGCTGGTGGAAAACATC 3′ forward; 5′ CTTCGTGTTCCTTGCACATC 3′ reverse; atrogin-1: 5′ GCAAACACTGCCACATTCTCTC 3′ forward; 5′ CTTGA GGGGAAAGTGAGACG 3′ reverse.

Retrieval and characterization of CD45+ infiltrating cells

Infiltrating cells were retrieved from damaged muscles at days 1, 3, 5, 7, 10, and 15 after injection of CTX. Muscles were dissociated by enzymatic digestion with collagenase type V (Sigma-Aldrich) (0.5 mg/ml) and dispase (Invitrogen) (3.5 mg/ml) at 37°C for 40 min. Infiltrating cells were further purified using CD45-conjugated magnetic beads (Milteny Biotec, GmbH). The purity was verified by flow cytometry after incubation with FITC-labeled anti-CD45.2 mAb (final concentration 5 μg/ml; BD Pharmingen, clone 104) and PE-labeled anti-F4/80 mAb (final concentration 5 μg/ml; AbD Serotec, clone CI:A3-1). Labeled cells were washed and analyzed by flow cytometry using FACS-Calibur flow cytometer and the Flow Jo Software v. 8.6.1 (Tree Star, Inc.). Purity was routinely >92%.

Western blot analysis

Both CD45+ infiltrating cells and whole muscle were lysed in Tris 10 m*M* pH 8.0, NaCl 150 m*M*, Nonidet P40 1%, sodium dodecyl sulfate 0.1%, EDTA 1 m*M*, and protease inhibitors cocktail [containing 4-(2-aminoethyl)benzenesulfonyl fluoride (AEBSF), pepstatinA, E-64, bestatin, leupeptin, and aprotinin; Sigma-Aldrich]. Lysates were centrifuged at 16,000 *g* for 5 min at 4°C. For Western blot analysis, equal amounts of protein (20 μg) were resolved by sodium dodecyl sulfate polyacrylamide gel electrophoresis and transferred onto Immobilon-P (Millipore). After Ponceau S (Sigma-Aldrich) staining, membranes were saturated in Tris-HCl 20 m*M*, pH 7.6, NaCl 150 m*M* (Tris-buffered saline [TBST]), containing nonfat milk 5% and Tween 20 0.1%. Antigens were detected using either rabbit polyclonal anti-Cu/Zn superoxide dismutase 1 (SOD1, final concentration 0.5 μg/ml; Assay Designs), or rabbit polyclonal anti-thioredoxin (Trx, final concentration 0.1 μg/ml; Abcam), mouse monoclonal anti-HMGB1 (final concentration 0.1 μg/ml, kindly provided by Dia.Pro. Diagnostic Bioprobes), mouse monoclonal anti-β-actin (final concentration 0.1 μg/ml; Sigma-Aldrich, clone AC15), or mouse monoclonal anti-GAPDH (final concentration 0.1 μg/ml; Sigma-Aldrich, clone GAPDH-71.1) antibodies. All antibodies were diluted in TBST 5% notfat milk. Incubation was performed overnight at 4°C for primary antibodies and 1 h at room temperature for the second-step reagents. Primary antibodies were revealed with HRP-conjugated secondary antibodies (final concentration 0.2 μg/ml; GE Healthcare Europe GmbH) and a chemiluminescence kit (ECL, Western blotting detection reagents; GE Healthcare Europe GmbH). To detect the microtubule-associated protein light chain 3 (LC3), we performed a pharmacological blockade of microtubules by intraperitoneal injection of colchicine (Sigma-Aldrich), which blocks autophagosome maturation to autolysosomes and prevents the degradation of LC3. The intraperitoneal treatment (0.4 mg/kg/day) was carried out the last 2 days exclusively before sacrifice. Frozen muscles were homogenized in sucrose 68 m*M*, KCl 50 m*M*, Tris HCl 50 m*M* pH 7.4, EDTA 10 m*M* pH 8, bovine serum albumin (BSA) 0.2% and protease inhibitors cocktail (containing AEBSF), pepstatinA, E-64, bestatin, leupeptin, and aprotinin; Sigma-Aldrich). Samples were incubated with mouse anti-LC3 mAb (final concentration 0.2 μg/ml; Nanotools) for 2 h at room temperature and with HRP-conjugated secondary antibody (final concentration 0.2 μg/ml) for 1 h at room temperature.

Immunofluorescence for HMGB1 and CD68

HMGB1 expression in healthy and damaged muscle (3 days after CTX injection) was assessed by immunofluorescence. The muscles were fixed in paraformaldehyde 4% and cryopreserved in sucrose 30% and then frozen in liquid nitrogen. Serial cryostal sections were washed with PBS, permeabilized with 0.1% Triton X-100, and blocked with 5% BSA in PBS in the presence or not of the specific HMGB1 inhibitory peptide (final concentration 1 μg/ml; Abcam) for 1 h at room temperature as a control. Then, sections were incubated with rabbit polyclonal anti-HMGB1 antibody (final concentration 2 μg/ml; Abcam) and/or with rat monoclonal anti-CD68 antibody (final concentration 2 μg/ml; AbD Serotec, clone FA-11) in PBS, 2% BSA overnight at 4°C. Sections were washed twice in PBS and then incubated with an Alexafluor 594-conjugated goat anti-rabbit Abs (final concentration 4 μg/ml; Invitrogen) and/or Alexafluor 488-conjugated anti-rat antibodies (final concentration 4 μg/ml; Invitrogen) for 1 h at room temperature. Sections were then incubated with Hoechst 33258 (final concentration 10 μg/ml, Invitrogen) for 10 min at room temperature.

HMGB1 expression by purified CD45+ cells was detected by immunofluorescence. Isolated CD45+ cells were seeded on polylysine-coated slides for 1 h at room temperature in PBS, 0.5% BSA, and 2 m*M* EDTA. For immunofluorescence, cells were fixed in acetone for 10 min at −20°C. Cells were washed with PBS, permeabilized with 0.1% Triton X-100, and blocked with 5% BSA in PBS for 1 h at room temperature. Cells were then incubated with polyclonal rabbit anti-HMGB1 (final concentration 12 μg/ml; AbD Serotec) in PBS, 2% BSA overnight at 4°C. Cells were washed twice in PBS and then incubated with an Alexafluor 594-conjugated goat anti-rabbit Abs (final concentration 4 μg/ml; Invitrogen) for 1 h at room temperature. Cells that were incubated with Hoechst 33258 (final concentration 10 μg/ml; Invitrogen) for 10 min at room temperature were mounted with glycerol and analyzed by confocal microscopy (Ultraview microscope).

Chemotaxis assay

Modified chemotaxis assays were performed using Boyden chambers (8): polycarbonate filters (8 μm pores; Neuro Probe, Inc.) were coated with porcine skin gelatin (2 mg/ml; Sigma-Aldrich). Lower chambers were loaded with DMEM (negative control), Dulbecco's modified Eagle's medium (DMEM) containing fetal calf serum (positive control), DMEM containing HMGB1 (HMGBiotec; 100 ng/ml), HMGB1 in reducing or oxidizing condition (DTT, 750 μM or H_2O_2, 25 μM), DTT, or H_2O_2 alone. Box A (HMGBiotec; 100 ng/ml) was added when indicated to assess the relative contribution of HMGB1 in the migration process. Upper chambers were loaded with 50,000 murine mesoangioblasts in the presence of DTT or H_2O_2. Boyden chambers were then incubated at 37°C in 5% CO_2 for 6 h. Cells on the upper section of the filters were mechanically removed. Mesoangioblasts that had migrated to the lower section of the filters were fixed with absolute ethanol, stained with Giemsa (Sigma-Aldrich), and counted in 10 randomly selected fields per filter.

Mesoangioblast differentiation in vitro

Murine mesoangioblasts, derived and propagated *in vitro* as described (50), were cultured (20,000 cells/well) in DMEM + 20% fetal calf serum (nonpermissive medium) at 37°C for 24 h in Matrigel-coated wells. To allow differentiation toward myofibers, mesoangioblast were treated with DMEM + 2% horse serum, plus insulin-like growth factor 1 (IGF) (Sigma-Aldrich) 50 ng/ml (permissive medium) in the absence or presence of DTT 750 μM or H_2O_2 25 μM. Cell viability was routinely assessed by Trypan blue exclusion and LDH release (not shown) into culture supernatants. After 4 days, differentiated mesoangioblasts were fixed in PFA 4% and stained with mouse anti-myosin heavy chain antibodies (final concentration 10 μg/ml; Developmental Studies Hybridoma Bank) followed by Alexafluor 488-conjugated anti-mouse antibodies (final concentration 4 μg/ml; Invitrogen). Nuclei were counterstained with Hoechst 33258 (final concentration 10 μg/ml; Invitrogen). Myotube number was evaluated by IN-cell analyzer.

Satellite cells retrieval and differentiation in vitro

Healthy muscles (TA and quadriceps) were dissociated in sterile condition by enzymatic digestion with collagenase type V (Sigma-Aldrich) (0.5 mg/ml) and dispase (Invitrogen) (3.5 mg/ml) at 37°C for 40 min, and then cells were plated in Ham's F10 medium (Sigma-Aldrich) + 20% HyClone fetal bovine serum defined (Thermo Scientific) and 2.5 mg/ml bFGF (PeproTech) (growth medium [GM]) for 1 h and 30 min at 37°C to allow fibroblast adhesion. Nonadhering cells, containing satellite cells, were retrieved, cells were plated on collagen (Sigma-Aldrich) and then propagated in GM for 4 days at 37°C as described (45). Satellite cells were then cultured (70,000 cells/well) in DMEM + 5% horse serum (permissive medium) in collagen-coated 12-well plates. DTT, 500 μM, or H_2O_2, 25 μM were added for 4 h in GM before switching the cells to permissive medium. Differentiation to myofibers was evaluated after 2 days. Cells were fixed in PFA 4% and stained with a mouse anti-myosin heavy-chain hybridoma supernatant (Ab final concentration 10 μg/ml; Developmental Studies Hybridoma Bank) followed by Alexafluor 488-conjugated anti-mouse Abs (final concentration 4 μg/ml; Invitrogen). Nuclei were counterstained with Hoechst 33258 (final concentration 10 μg/ml; Invitrogen). Myotube number was evaluated by IN-cell analyzer.

Statistics

Data are expressed as means ± SEM. Statistical analysis was performed using Student's *t*-test for unpaired data or one-way ANOVA followed by a Dunnett's or Newman-Keuls *post hoc* test when appropriate. Values of $p < 0.05$ were considered statistically significant.

Results

Muscle regeneration is accompanied by a heightened antioxidant response

We triggered skeletal muscle injury and regeneration by injection of CTX into the TA muscle. Figure 1 shows that lysis of most fibers occurs in the area of injection within a day (Fig. 1B), followed by massive infiltration by inflammatory cells (Fig. 1C and D, 3 and 7 days after injury, respectively). Satellite cell proliferation and fusion conincide with the formation of new fibers, which can be easily identified by the central distribution of the nuclei (Fig. 1E, 10 days after injury). The tissue eventually heals (15 days after injury, Fig. 1F).

To investigate whether muscle injury is accompanied by a heightened reducing microenvironment, we assessed the presence, kinetics, and distribution of oxidizing species (H_2O_2) and of NPSH (GSH and cysteine), using specific probes (PG1 and Mercury Orange, respectively). As shown in Figure 1G, no PG1 signal is present in the healthy muscle, indicating that ROS are under the detection limits and that no detectable oxidative stress is identified. In contrast, a strong positivity for PG1 is observed in the injured muscle, peaking at day 1 after CTX injection sustained for at least 3 days (Fig. 1H, I). Virtually, no green-fluorescent signal is detectable at later times (10 and 15 days from injury) when tissue remodeling and active regeneration prevail (Fig. 1K, L). H_2O_2 production is clearly associated with damaged fibers. Infiltrating leukocytes are only faintly stained by PG1, indicating that they do not substantially contribute to the oxidative stress.

Unlike PG1, Mercury Orange staining of NPSH is mildly positive in healthy muscles (Fig. 1M). After injury, the Mercury Orange signal progressively increases, with a slightly delayed kinetics when compared with PG1 staining. Regenerating fibers display the most intense fluorescence 3 days after damage (Fig. 1O). At this time, infiltrating leukocytes are strongly stained by Mercury Orange, suggesting at this point that they contribute to the production of NPSH (Fig. 1O). NPSH staining is still higher than in healthy muscles after 7 days and decreases thereafter to levels at or below the background (Fig. 1P–R).

Costaining of PG1 and Mercury Orange at day 3 (Fig. 2) provides additional information. First, the same injured fibers are positive for both PG1 (Fig. 2A, B) and Mercury Orange (Fig. 2A, D), indicating that fibers undergoing an oxidative response react to the increased ROS generation by increasing the production of antioxidant species. Second, highly damaged fibers (arrows) retain a strong ROS-associated positivity, whereas in less injured fibers (arrowheads) the antioxidant response predominates. Interestingly, in costained fibers, the intracellular staining of ROS and NPSH is only partially overlapping.

The specificity of the ROS and NPSH staining is confirmed by the experiment shown in Figure 2C and E. ROS staining by PG1 is prevented by incubating muscle sections with the reducing agent DTT that quenches ROS (Fig. 2C). Mercury Orange staining is prevented by treatment of muscle sections with N-ethylmaleimide, which blocks free thiols (Fig. 2E).

Mitochondria contribute to damage-induced ROS production

To identify the intracellular sources of ROS, muscle sections at different times after injury were simultaneously stained with the ROS probe H_2DCFDA and the mitochondria-selective dye, mitotracker. As shown in Figure 3A, healthy muscle fibers exhibited a strong mitochondrial signal, mostly restricted to the periphery of the fibers (arrowheads). As expected, ROS production is below the level of detection (Fig. 3B). At 12 h from the injury (Fig. 3C, D), less damaged fibers

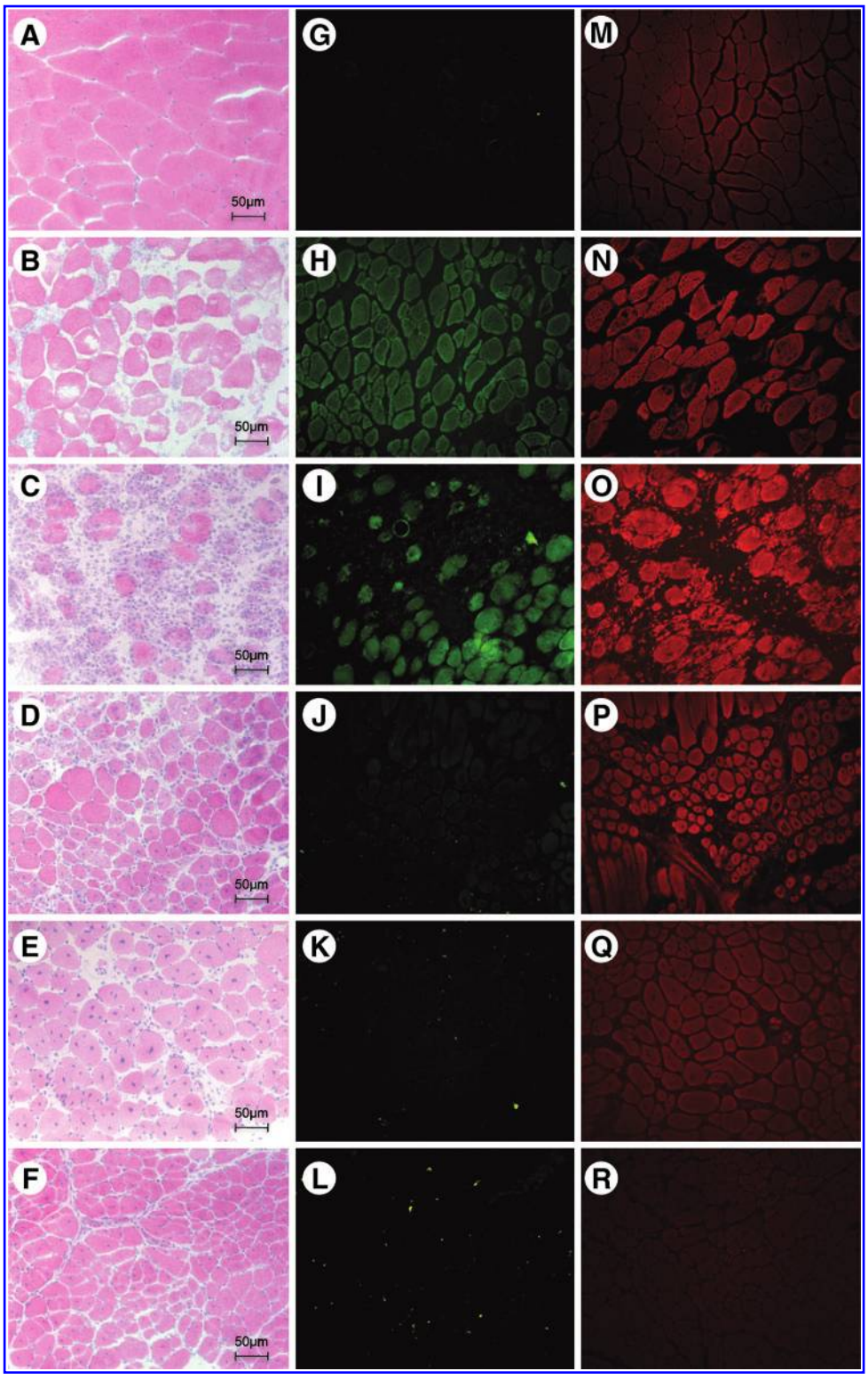

FIG. 1. Oxidative stress and antioxidant response in acutely damaged and regenerating muscle. Skeletal muscles acutely damaged by injection of cardiotoxin (CTX) were retrieved immediately before **(A, G,** and **M)** and 1 **(B, H,** and **N)**, 3 **(C, I,** and **O)**, 7 **(D, J,** and **P)**, 10 **(E, K,** and **Q),** and 15 **(F, L,** and **R)** days after damage. Representative hematoxylin and eosin stains are shown **(A–F)**. Extensive necrosis is evident after 1 day **(B)**, mononuclear infiltrates are prominent between 3 and 7 days **(C, D)**, and regenerating fibers are clearly detectable at days 10 and 15 **(E, F)**. Consecutive muscle sections were stained with peroxy green (PG1) to detect hydrogen peroxide (H_2O_2) production **(G–L)** and Mercury Orange to detect free nonprotein thiols **(M–R)** and analyzed by fluorescence microscopy. Magnification 60×. Scale bars: 50 μm.

display a peripheral mitochondrial signal, which is actually stronger than in healthy fibers (Fig. 3C, arrowheads). Moreover, mitochondria apparently redistribute diffusing to nonsubsarcolemmatic cytoplasmic domains, where they appear as isolated fluorescent dots (arrows). At this time, DCF staining colocalizes with mitochondria, both at the periphery of the fibers (Fig. 3D, arrowheads) and inside (Fig. 3D, arrows). The colocalization of mitochondrial and ROS probes is easily appreciated at the higher magnification shown in Figure 3G–I. Twenty-four hours after injury, only some fibers display an evident mitochondrial net (Fig. 3E, arrow), which is completely lost in other fibers (Fig. 3E, arrowhead). ROS-associated fluorescence is abundant at this time. However, the colocalization with mitochondria is largely lost (Fig. 3F,

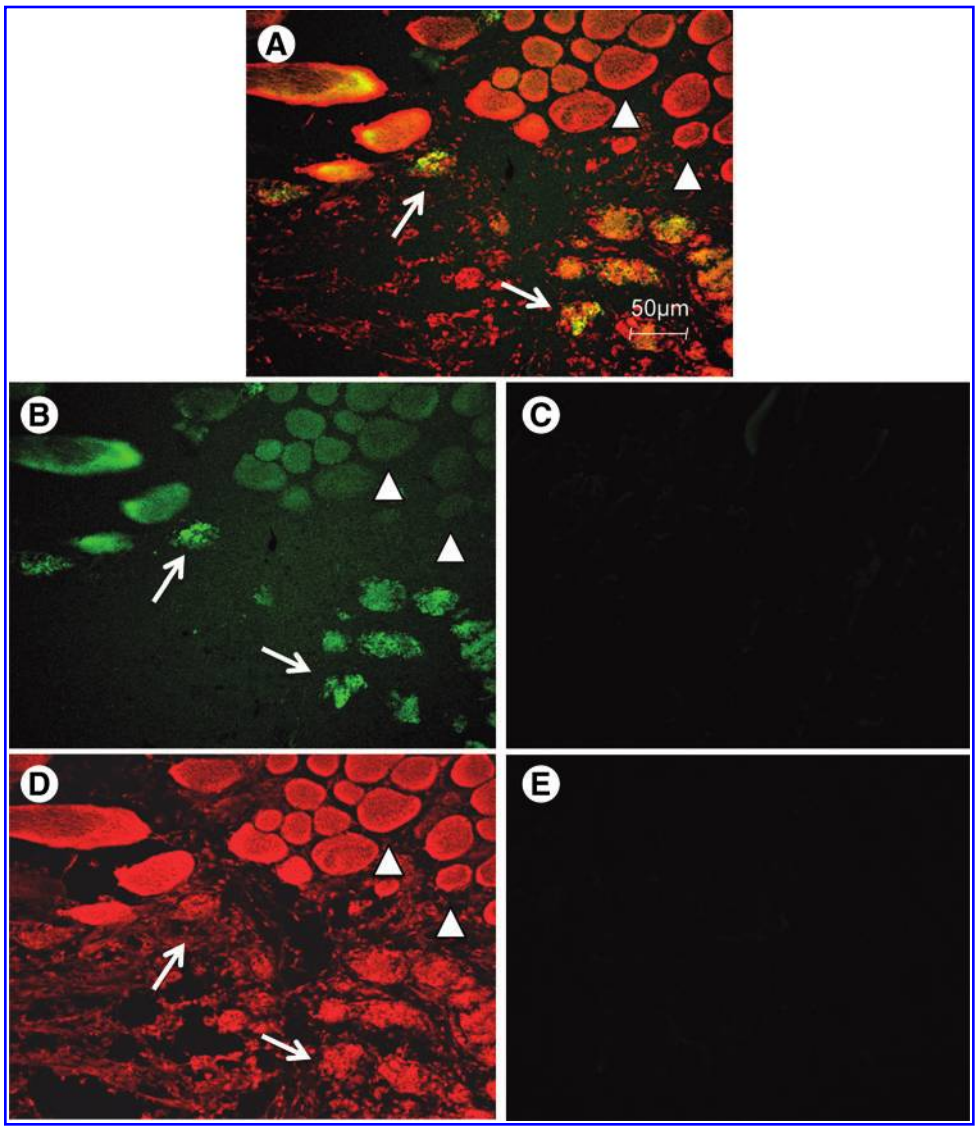

FIG. 2. Double staining with PG1 and Mercury Orange at day 3 after damage. Sections of muscle retrieved 3 days after damage were costained with PG1 **(A, B)** and Mercury Orange **(A, D)**. As a control, PG1 staining was prevented by neutralization of reactive oxygen species (ROS) by preincubation of muscle sections with 1 m*M* dithiothreitol (DTT) for 10 min. **(C)** Mercury Orange staining was prevented by blocking thiol groups with 100 μM N-ethylmaleimide for 10 min **(E)**. The sections were analyzed by confocal microscopy, and images were acquired with Fluoview FV500 software. Magnification 60×. Scale bars: 50 μm. Highly damaged fibers were identified by *arrows*, whereas less injured fibers were identified by *arrowheads*.

asterisk, arrowhead). Less than 5% of the fibers still express both mitochondrial- and ROS-associated fluorescence signals (arrows). Most of the DCF staining is diffuse, indicating a nonmitochondrial origin of the ROS.

To better evaluate the changes in mitochondrial homeostasis, muscle tissues were analyzed by electron microscopy at various times after injury (Fig. 4). Results confirm that mitochondria undergo a dramatic reorganization as a consequence of CTX-induced skeletal muscle injury, with evidence of mitophagy at earlier phases of the process (see Fig. 4B, C) and progressive reconstitution of the organelles at later phases of tissue regeneration (Fig. 4D–F). The involvement of the mitophagic process in the fate of mitochondria is also suggested by the expression after damage at day 3 of LC3-II, a surrogate marker of autophagosome formation (Fig. 4I). The proteasome is also involved in regulating mitochondrial architecture and dynamics (30, 52). In keeping with this notion, CTX treatment upregulates the expression of the two ubiquitin ligases, MuRF1 and atrogin-1, which on day 1 after injury display mRNA levels approximately 2- and 4-fold those present in untreated muscles, respectively. mRNA levels of these genes dropped in the days after injury (Fig. 4G, H).

Regenerating muscle fibers and infiltrating leukocytes upregulate antioxidant enzymes

To better characterize the relative contribution of muscle fibers and infiltrating cells to the redox remodeling in the injured/regenerating muscle, we isolated CD45+ leukocytes from the tissue at various times after injury and compared the expression of antioxidant enzymes, such as the ROS scavenger, SOD1 and the oxidoreductase, Trx, in CD45+ leukocytes and in muscle lysates. Figure 5 shows that leukocytes infiltrate the muscle early, being already abundant a day after injury ($2.38 \pm 0.52 \times 10^6$/mouse), peaking at 3 days ($3.15 \pm 0.83 \times 10^6$/mouse), and still heavily infiltrating the tissue for up to 7 days (Fig. 5A). Most of the CD45+ infiltrating cells are monocytes/macrophages, as demonstrated by the expression of the F4-80 membrane marker (Fig. 5B). The expression of SOD1 and Trx by infiltrating leukocytes is already elevated after a day. Elevated levels of SOD1 are sustained through day 15. Trx expression decreases at day 10, even if it remains higher than that observed in circulating leukocytes (Fig. 5C).

Muscle lysates from healthy muscles express SOD1 and low levels of Trx (Fig. 5D). The expression of SOD1 decreases

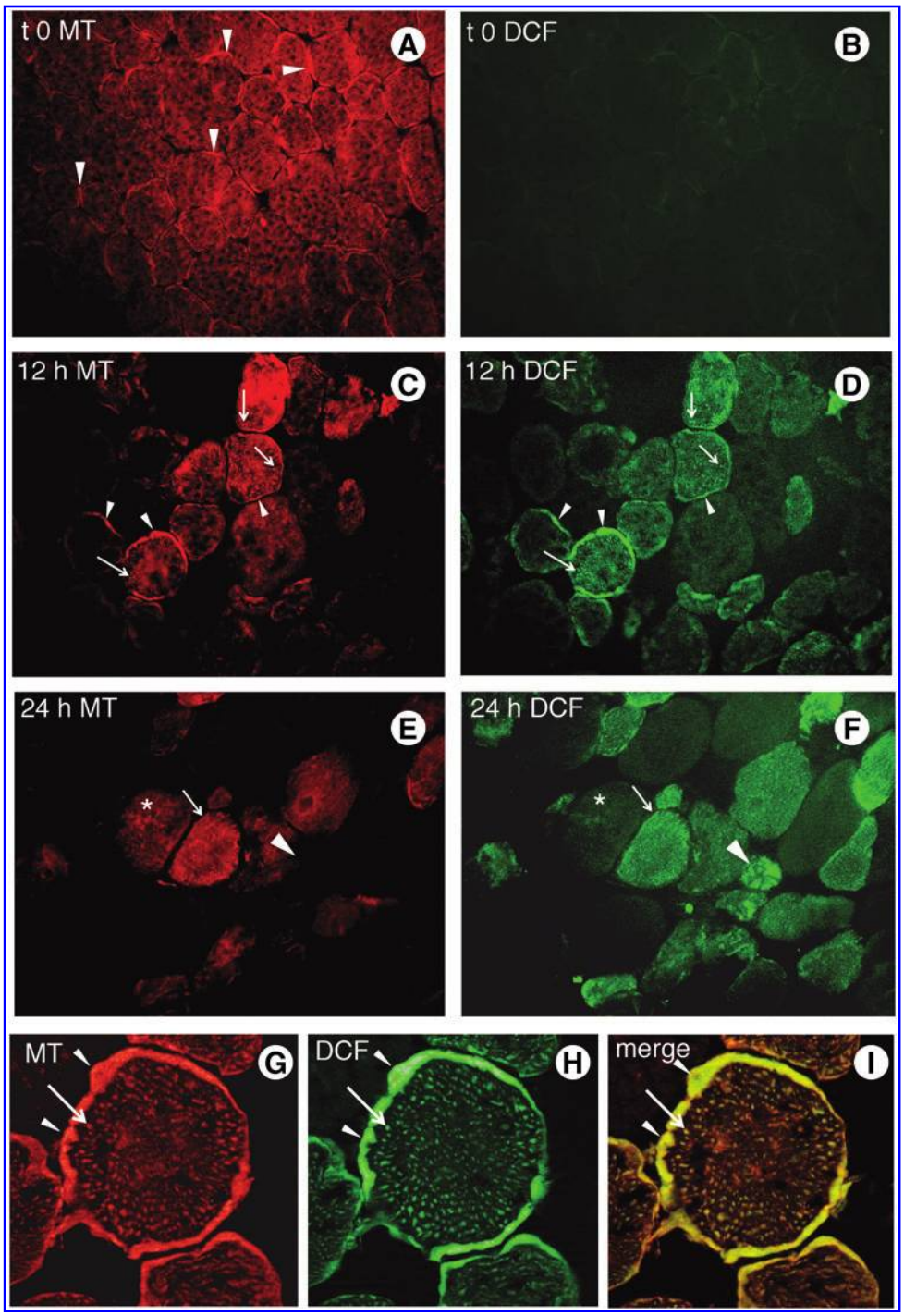

FIG. 3. Mitochondria are only associated with ROS generation during the early phases of muscle damage/ regeneration. Skeletal muscle was retrieved immediately before **(A, B)**, and then at 12 h **(C, D, G–I)** and 24 h **(E, F)** after injury and stained with Mitotracker **(***red color, panels* **A, C, E, G, I)** or DCF-DA **(***green color, panels* **B, D, F, H, J)**. **(A)** *Arrowheads:* mitochondrial signal. **(C, D, G–I)** coexistence of mitochondrial and DCF signals under the sarcolemma (*arrowheads*) and in intracellular dots (*arrows*). **(E, F)** coexistence of mitochondrial and DGF signal is evident in less damaged fibers (*arrows*) and is progressively lost in more damaged ones (*arrowheads and asterisk*). **(A–F)**: 40× **(G–I)**: 100× magnification.

at day 1 after injury, when the oxidative insult is maximal (see also Fig. 1) and increases at later times, characterized by extensive muscle regeneration. At these time points, the expression of Trx is also clearly upregulated. Trx expression in fully regenerated muscles drops back to levels comparable to healthy muscles (Fig. 5D).

Infiltrating cells deliver HMGB1 to the damaged muscle

The expression of HMGB1, a key signaling molecule connecting injury with regeneration, was analyzed in both muscle fibers and CD45+ leukocytes at various time points after damage. As shown in Figure 6, HMGB1 is barely detectable in healthy skeletal muscle tissue (Fig. 6B, C, G) where it is restricted to the peripheral nuclei (Fig. 6C, G). HMGB1 is abundant in the injured muscle at day 3 after damage, where it spreads diffusely within the damaged fibers (Fig. 6E, F, G). HMGB1 levels remain elevated till late time points after damage (Fig. 6G). Moreover, HMGB1 is highly expressed by infiltrating CD45+ leukocytes at various time points after damage (Fig. 6H). Interestingly, HMGB1 expression in CD45+ leukocytes isolated from injured muscles is almost completely cytosolic (Fig. 6I–N), a distribution compatible with translocation into secretory vesicles and release. The

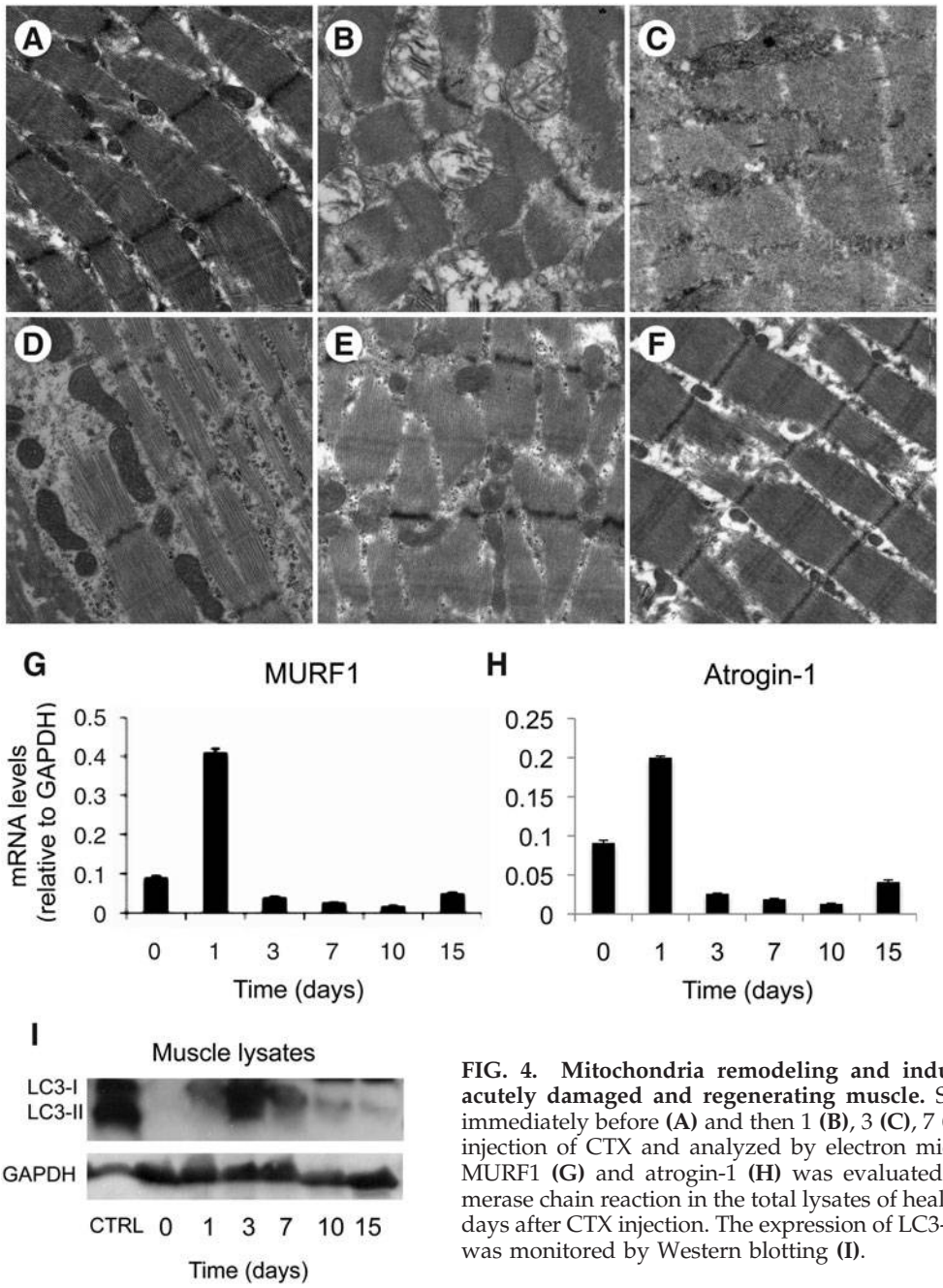

FIG. 4. Mitochondria remodeling and induction of ubiquitin ligases in acutely damaged and regenerating muscle. Skeletal muscles were retrieved immediately before **(A)** and then 1 **(B)**, 3 **(C)**, 7 **(D)**, 10 **(E),** and 15 **(F)** days after injection of CTX and analyzed by electron microscopy. mRNA expression of MURF1 **(G)** and atrogin-1 **(H)** was evaluated by reverse transcriptase–polymerase chain reaction in the total lysates of healthy muscles 0, 1, 3, 7, 10, and 15 days after CTX injection. The expression of LC3-II at various times after damage was monitored by Western blotting **(I)**.

specificity of HMGB1 staining is confirmed by the experiment shown in Supplementary Figure S1 (Supplementary Data are available online at www.liebertonline.com/ars). HMGB1 staining (red color) is prevented by incubating muscle sections retrieved at day 3 after damage with the specific HMGB1 inhibitory peptide (Supplementary Fig. S1).

Muscle regeneration largely depends on the ability of stem and precursor cells to reach the site of damage, proliferate and fuse, events that are believed to be favored by HMGB1 (42). We, therefore, determined whether changes in the redox state of the tissue microenvironment influence HMGB1-mediated migration of vessel-associated stem cells, mesoangioblasts. As shown in Figure 7, recombinant purified HMGB1 elicits mesoangioblast migration *in vitro*, as verified using a Boyden apparatus, to a level comparable to that obtained with the positive control (Fig. 7A). Migration is maintained under reducing conditions generated by the addition of 750 μM DTT (Fig. 7B, filled columns), whereas it abates in the presence of 25 μM H_2O_2 (Fig. 7B, empty columns). Migration is inhibited in the presence of the N-terminal fragment of HMGB1 (box A), which behaves as a HMGB1 antagonist (Fig. 7B).

In the presence of IGF1, mesoangioblasts efficiently differentiate *in vitro* toward myofibers (Fig. 7D). Differentiation in response to IGF1 is maintained under reducing conditions generated by the addition of 750 μM DTT (Fig. 7E), whereas the presence of 25 μM H_2O_2 restricts their ability to differentiate (Fig. 7F). Cell viability was consistently >95% in all experimental conditions (not shown). Quantification shows that within an oxidizing environment, the numbers of both myosin heavy-chain positive (MyHC+) cells and of myofibers

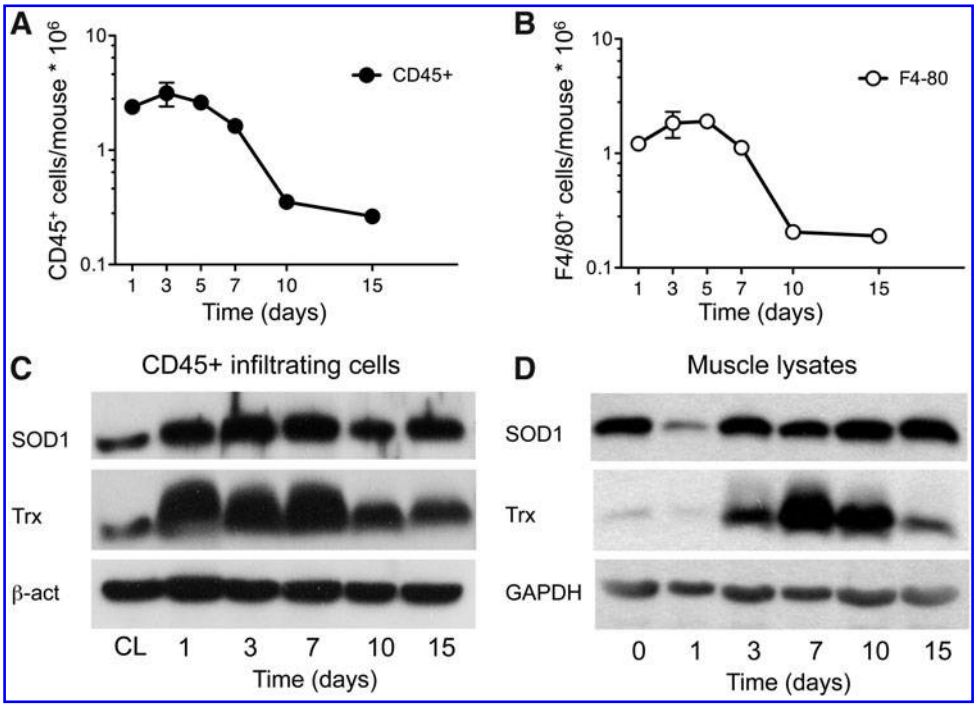

FIG. 5. Antioxidant response in damaged fibers and infiltrating mononuclear cells. CD45+ **(A)** and of F4/80+ **(B)** cells (absolute number, ordinant) were retrieved after enzymatic digestion of skeletal muscle at subsequent time points after CTX injection (days, abscissa). Results represent the means ± SD of 3 independent experiments. The expression of superoxide dismutase 1 (SOD1) (*upper panels*) and thioredoxin (Trx, *middle panels*) was evaluated by Western blotting in CD45+ cells **(C)** retrieved from peripheral blood (circulating leukocytes [CL]) or from muscle 1, 3, 7, 10, and 15 days after CTX injection and in the total lysates **(D)** of healthy muscles 0, 1, 3, 7, 10, and 15 days after CTX injection. The expression of housekeeping genes was evaluated in the *lower panels*.

with more than 4 nuclei were significantly decreased (Fig. 7G) to a level comparable to that observed in the absence of the differentiating agent, IGF1. A similar result was also obtained using muscle-resident stem cells, the satellite cells. As depicted in Figure 8 satellite cells spontaneously differentiate in myofibers in the presence of horse serum (Fig. 8A). Satellite cell differentiation, measured as number of MyHC+ myofibers with >4 nuclei, is maintained in the presence of DTT (500 μM, Fig. 8B) and inhibited by H_2O_2 (25 μM, Fig. 8C). Quantification is presented in Figure 8D.

Discussion

Acute injury of skeletal muscle initiates a tightly regulated homeostatic response, involving recruitment of inflammatory leukocytes and activation of local stem cells that proliferate and fuse, yielding novel fibers. The actual molecular mechanisms regulating these events are only partially understood (7, 59). We have followed the temporal response to injury in muscle fibers and observed that successful regeneration is associated with a dramatic and highly regulated redox response. ROS generation occurs in the damaged muscle soon after injury, followed rapidly by both an intra- and extracellular propagation of an antioxidant response promoting muscle regeneration and remodeling.

Consistent with mitochondria being the major source of ROS in eukaryotic cells (21, 46, 52), our findings demonstrate that CTX injection results in rapid ROS production by mitochondria. Mitochondrial ROS overproduction likely leads to oxidation of the sarcomeric proteins and impairment of cell viability (2), thereby contributing to the CTX-induced injury. Moreover, mitochondria themselves have been proposed to be major targets of the oxidative insult provided by ROS (11), suggesting that the dramatic dysfunction of mitochondria observed between 12 and 24 h after injury is dependent, at least in part, on the heightened production of ROS by these organelles. ROS produced by injured mitochondria can trigger mitophagy that, on eliminating damaged mitochondria and oxidized proteins, supports survival. The induction of mitophagy is supported by the observation that a marker of autophagosome formation, LC3-II, is expressed in the damaged muscle by 3 day after injury, perhaps prompted by HMGB1 production by recruited leukocytes. In addition, we show here that the acute skeletal muscle injury triggered by CTX injection results in the induction of the ubiquitin E3 atrophy markers, muscle RING finger-1 (MURF1 or TRI63) and muscle atrophy F-Box (known as MAFbx, atrogin-1) (36, 63) These proteins are hallmarks of the activation of the ubiquitin-proteasome pathway underlying muscle atrophy related to disuse or cachexia (43, 53). Our finding that these genes are upregulated during the initial phase of acute muscle damage and regeneration suggests that protein catabolism through the proteasome machinery is also acting in this setting and supports the observation that ubiquitination is required for eliminating damaged mitochondria (28).

Interestingly, ROS production persists even when mitochondria are completely destroyed, indicating that other cellular sources other than mitochondria predominate at later times. The diffuse staining of ROS observed at day 3 after injury suggests that, similar to other cell systems, cytoplasmic enzymes, such as NADPH oxidase (29) and dual oxidase (37), are involved in ROS generation. Since ROS-mediated mitochondrial biogenesis has been demonstrated in skeletal muscle (11), it is conceivable that the persistent production of ROS may also contribute to the progressive reconstitution of the organelles at later phases of tissue regeneration.

Soon after the generation of increased ROS, an antioxidant response is triggered in injured muscles, as indicated by the increased staining with Mercury Orange, a dye that specifically binds NPSH, such as GSH and cysteine itself. GSH is the

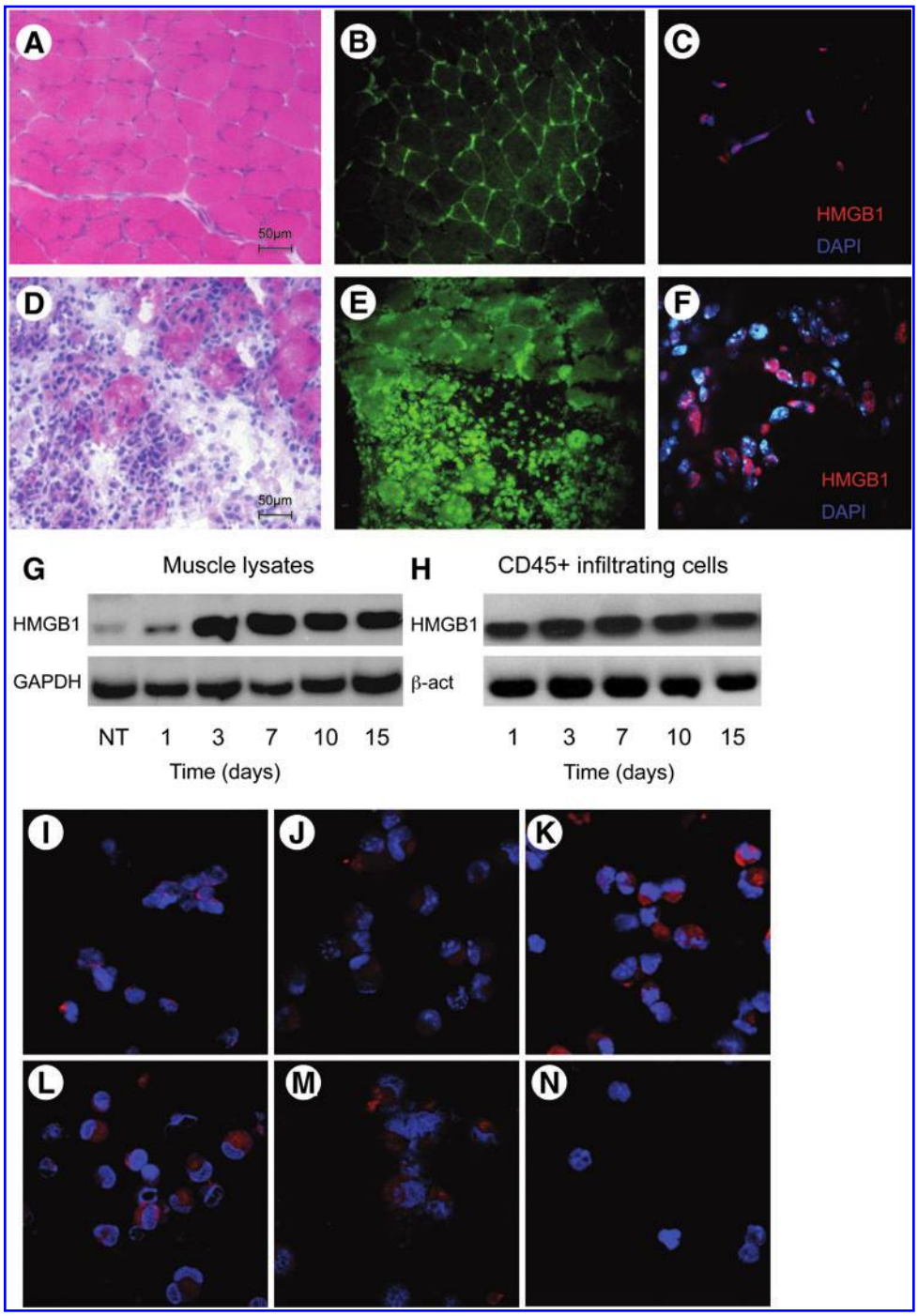

FIG. 6. High-mobility group box 1 (HMGB1) detection in damaged fibers and infiltrating mononuclear cells. Sections of healthy muscle **(A–C)** or muscles retrieved 3 days after CTX injection **(C–F)** were stained with hematoxylin and eosin **(A** and **D)**, with anti-HMGB1 Abs (*green color panels* **B** and **E** and *red color*, *panels* **C** and **F**), and with the nuclear dye Hoechst (*blue color*, *panels* **C** and **F)**. After staining, sections were analyzed by confocal microscopy. Magnification 60×. Scale bar: 50 μm. HMGB1 expression was evaluated by Western blotting in the total lysates **(G)** of healthy muscles (NT) and 1, 3, 7, 10, and 15 days after CTX injection and in CD45+ cells **(H)** retrieved from muscle 1, 3, 7, 10, and 15 days after CTX injection. Subcellular localization of HMGB1 in CD45+ cells retrieved from damaged muscle 1 **(I)**, 3 **(J)**, 7 **(K)**, 10 **(L),** and 15 **(M)** days after CTX injection was evaluated by confocal microscopy after staining with anti-HMGB1 Abs (*red color*) and Hoechst (*blue color*). As a control, primary anti-HMGB1 Abs was omitted in CD45+ cells retrieved from damaged muscle 3 days after CTX injection **(N)**.

major non enzymatic antioxidant system in all cell types. Reduced cysteine is particularly relevant in this context, as it is released in response to oxidative stress and induces a reduced state within the extracellular environment (49, 58, 62). Kinetic studies revealed that the highest production of ROS in muscle fibers occurs at day 1 after injury. ROS generation is sustained for 2 days and rapidly decreases thereafter. In contrast, the antioxidant response peaks later (day 3 after injury) and is maintained until regeneration and remodeling is complete. An interesting result, arising from the confocal microscopic analysis, is that the same fibers stain with reagents specific for both H_2O_2 and for NPSH, indicating that the antioxidant response takes place in the same damaged fiber where the ROS are produced. This finding also suggests that NPSH do not (or at least not completely) neutralize ROS directly, but rather protect molecular targets of ROS from oxidation.

The dynamic redox response in the damaged/regenerating muscle is not only due to redox-related events taking place within the injured fibers, but rather a significant contribution is also provided by the rapidly recruited and infiltrating leukocytes. In addition to NPSH, the ROS scavenger SOD1 and the oxido-reductase Trx are also upregulated, in both muscle tissue and infiltrating leukocytes. We focused on these two enzymes, as they are validated markers of the antioxidant response in both muscle and leukocytes (25, 49). SOD1 defective mice, in particular, represent a

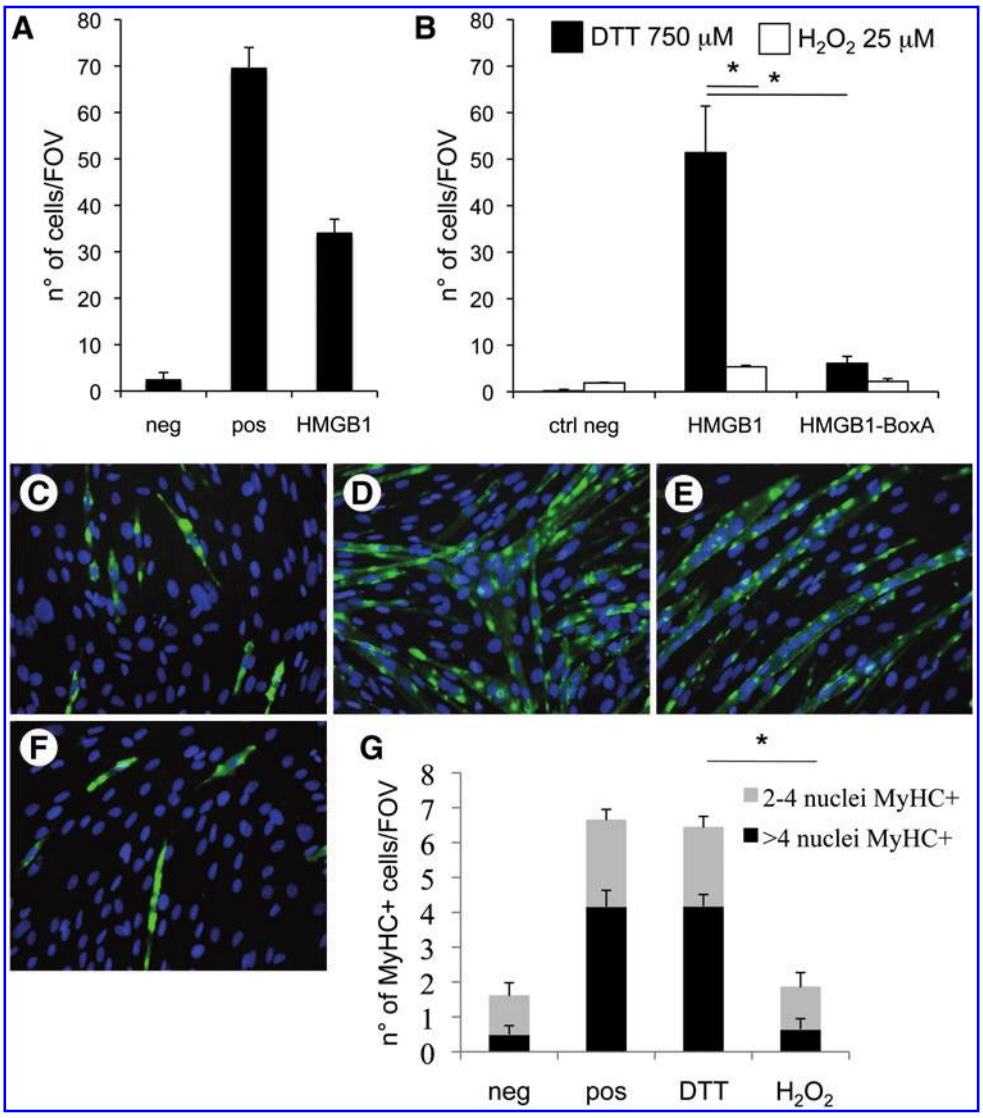

FIG. 7. ***In vitro*** **migration and differentiation of vessel associated stem cells in response to HMGB1.** Vessel associated stem cell migration was evaluated in response to negative (neg) and positive (pos) control media and to HMGB1 **(A)**. The migration of cells maintained under reducing conditions generated by the addition of 750 μM DTT (*filled columns*) or in oxidizing conditions with addition of 25 μM H_2O_2 (*empty columns*) was also evaluated in the presence or absence of the N-terminal fragment of HMGB1 (Box A), which behaves as a HMGB1 antagonist **(B)**. Migration was assessed in a modified Boyden chamber assay, evaluating the number of migrating cells for field of view (number of cells/FOV, ordinant). Bars represent mean ± SEM of three independent experiments. *Statistically significant values ($p < 0.05$). Ability of vessel associated stem cells to differentiate into myofibers was evaluated under nonpermissive **(C)** or under permissive **(D)** culture conditions and in permissive media under reducing **(E)** and oxidizing **(F)** conditions. Differentiation was evaluated, monitoring the expression of myosin heavy chain (*green color*) and the number of nuclei stained with the nuclear dye Hoechst per myofiber (*blue color*). The quantification of the number of myofibers (number of MyHC+ cells, ordinate) expressing 2–4 nuclei (gray bar) or >4 nuclei (black bar) is also reported **(G)**. Bars represent mean ± SEM of three independent experiments. *Statistically significant values ($p < 0.05$).

well-characterized model to study the role of chronic oxidative stress. They have constitutive sarcopenia, which is associated with progressive mitochondrial bioenergetic dysfunction as a consequence of persistent and sustained generation of ROS, thus indicating a protective role for antioxidants in physiologic conditions maintaining skeletal muscle integrity (24). Moreover, Trx is actively externalized by activated leukocytes, including monocytes, dendritic cells, and B lymphocytes, and occurs coincident with the switch in the extracellular redox state from the "resting" oxidized state to the "reduced" activated state in many innate and adaptive immunity responses (49, 62) as well as in the setting of cancer (44).

Although most fibers costain for ROS and NPSH, the ratio of the relative green and red fluorescence differs. Mercury Orange staining is stronger in less injured fibers, indicating that the most severely damaged fibers could, thus, undergo exhaustion of the antioxidant defense mechanisms and eventually succumb to oxidative stress, whereas the less damaged fibers have an opportunity to survive. Indeed, a role for oxidation in the regulation of skeletal muscle sustained during an acute injury, and conversely a protective action of exogenous anti-oxidants during normal physiology is well established (15, 22, 35, 40, 43, 53). The heightened and sustained antioxidant response taking place in stressed fibers generates a reducing microenvironment at the site of injury that may favor DAMP-induced muscle regeneration. The notion that a reducing extracellular microenvironment promotes DAMP activity is based on the evidence that many DAMPs, including HMGB1, are inactivated by oxidation (26, 31, 32, 61). Some other DAMPs may also play a role in the regulation of the inflammatory response to acute muscle injury, including members of the S100 family. S100A8, for example, undergoes redox-mediated modifications that affect its inflammatory properties, in particular its ability to attract leukocytes to sites of inflammation (9, 23, 48). Remarkably, we also found that infiltrating leukocytes and, to a lesser extent, damaged muscle fibers express HMGB1, one of the

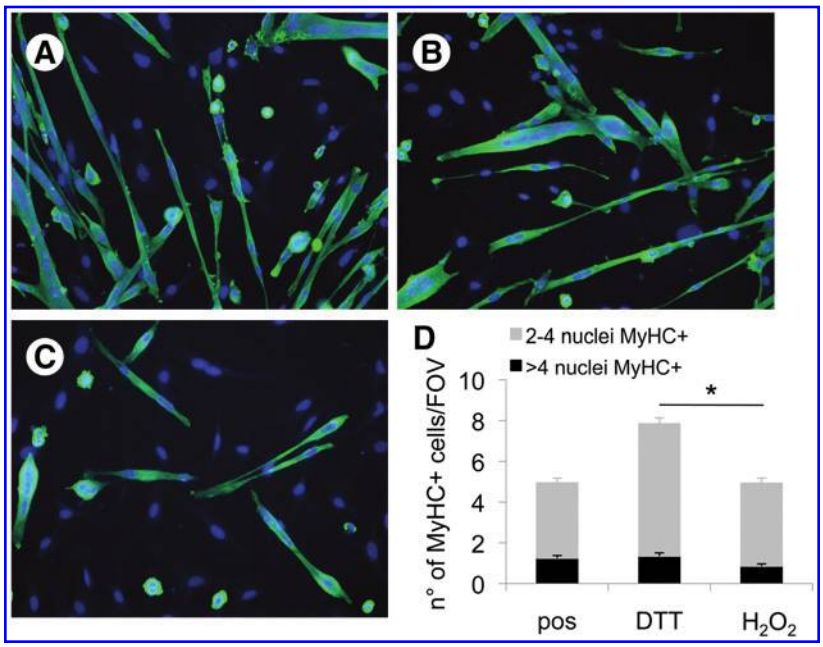

FIG. 8. Satellite cell differentiation toward myofibers *in vitro*. The ability of satellite cells to differentiate into myofibers was evaluated in permissive **(A)** culture media and in permissive culture media under reducing **(B)** and oxidizing **(C)** conditions. Differentiation was evaluated monitoring the expression of myosin heavy chain (*green*) and the number of nuclei stained with the nuclear dye Hoechst per myofiber (*blue*). The quantification of the number of myofibers (number of MyHC+ cells, *y*-axis) expressing 2–4 nuclei (gray bar) or > 4 nuclei (black bar) is also reported **(D)**. Bars represent mean ± SEM of three independent experiments. *Statistically significant values ($p < 0.05$).

best-characterized molecules involved in muscle healing (16). It is conceivable that HMGB1, weakly expressed by healthy muscle cells (16), is released by dying muscle cells soon after injury in low amounts but sufficient to recruit inflammatory cells. In contrast, sustained HMGB1 secretion, such as that observed in chronic inflammatory myopathies, is involved in the development of muscle weakness (20). We hypothesize that early release of HMGB1 by recruited inflammatory cells promotes stem cell proliferation and maintains their function while actual healing is accomplished, days after the initial injury.

An oxidizing environment within the damaged muscle would rapidly inactivate HMGB1, jeopardizing repair of the initial injury. Conversely, the reducing microenvironment generated by the potent antioxidant response to the oxidative insult provided by the initial damage can maintain the reducing activity of HMGB1, thereby prolonging its bioactivity. In addition, a reduced microenvironment may promote differentiation of precursor and stem cells into myofibers, as observed when mild oxidation of the medium inhibits this process.

In conclusion, we propose that the potent antioxidant response to ROS production in both muscle cells and recruited inflammatory cells is not only aimed at preventing possibly deleterious oxidative stress but also at restoring redox homeostasis. This also serves a signaling function, including the preservation of HMGB1 extracellular reducing capability necessary for a successful muscle regeneration. Further work is warranted to verify whether a relative failure of the antioxidant response contributes to the defective healing of dystrophic muscle, and whether this pathway may be a suitable target in patients with dystrophia. Experimental models with genetic disruption of key molecules in the anti-oxidant response, either in wild-type or dystrophic backgrounds, would be a valuable tool to accomplish this goal.

Acknowledgments

This work was supported by the Ministero della Salute (FIRB-IDEAS) to PR-Q, by the EU (Endostem) to S.B. and P.R.-Q., by the AFM to P.R.-Q. and S.B., and by the MIUR (PRIN 2008) to A.A.M. and P.R.-Q.

Author Disclosure Statement

No competing financial interests exist.

References

1. Arnold L, Henry A, Poron F, Baba-Amer Y, van Rooijen N, Plonquet A, Gherardi RK, and Chazaud B. Inflammatory monocytes recruited after skeletal muscle injury switch into antiinflammatory macrophages to support myogenesis. *J Exp Med* 204: 1057–1069, 2007.
2. Bayeva M and Ardehali H. Mitochondrial dysfunction and oxidative damage to sarcomeric proteins. *Curr Hypertens Rep* 12: 426–432, 2010.
3. Bell CW, Jiang W, Reich CF, 3rd, and Pisetsky DS. The extracellular release of HMGB1 during apoptotic cell death. *Am J Physiol Cell Physiol* 291: C1318–C1325, 2006.
4. Bianchi ME. DAMPs, PAMPs and alarmins: all we need to know about danger. *J Leukoc Biol* 81: 1–5, 2007.
5. Biscetti F, Straface G, De Cristofaro R, Lancellotti S, Rizzo P, Arena V, Stigliano E, Pecorini G, Egashira K, De Angelis G, Ghirlanda G, and Flex A. High-mobility group box 1 protein promotes angiogenesis after peripheral ischemia in diabetic mice through a VEGF-dependent mechanism. *Diabetes* 59: 1496–1505, 2010.
6. Bonaldi T, Talamo F, Scaffidi P, Ferrera D, Porto A, Bachi A, Rubartelli A, Agresti A, and Bianchi ME. Monocytic cells hyperacetylate chromatin protein HMGB1 to redirect it towards secretion. *EMBO J* 22: 5551–5560, 2003.
7. Brunelli S and Rovere-Querini P. The immune system and the repair of skeletal muscle. *Pharmacol Res* 58: 117–121, 2008.
8. Campana L, Bosurgi L, Bianchi ME, Manfredi AA, and Rovere-Querini P. Requirement of HMGB1 for stromal cell-derived factor-1/CXCL12-dependent migration of macrophages and dendritic cells. *J Leukoc Biol* 86: 609–615, 2009.
9. Carta S, Castellani P, Delfino L, Tassi S, Vene R, and Rubartelli A. DAMPs and inflammatory processes: the role of redox in the different outcomes. *J Leukoc Biol* 86: 549–555, 2009.

10. Castellani P, Angelini G, Delfino L, Matucci A, and Rubartelli A. The thiol redox state of lymphoid organs is modified by immunization: role of different immune cell populations. *Eur J Immunol* 38: 2419–2425, 2008.
11. Chang JC, Kou SJ, Lin WT, and Liu CS. Regulatory role of mitochondria in oxidative stress and atherosclerosis. *World J Cardiol* 2: 150–159, 2010.
12. Chavakis E, Hain A, Vinci M, Carmona G, Bianchi ME, Vajkoczy P, Zeiher AM, Chavakis T, and Dimmeler S. High-mobility group box 1 activates integrin-dependent homing of endothelial progenitor cells. *Circ Res* 100: 204–212, 2007.
13. Chazaud B, Brigitte M, Yacoub-Youssef H, Arnold L, Gherardi R, Sonnet C, Lafuste P, and Chretien F. Dual and beneficial roles of macrophages during skeletal muscle regeneration. *Exerc Sport Sci Rev* 37: 18–22, 2009.
14. Ciciliot S and Schiaffino S. Regeneration of mammalian skeletal muscle. Basic mechanisms and clinical implications. *Curr Pharm Des* 16: 906–914, 2010.
15. Dargelos E, Brule C, Stuelsatz P, Mouly V, Veschambre P, Cottin P, and Poussard S. Up-regulation of calcium-dependent proteolysis in human myoblasts under acute oxidative stress. *Exp Cell Res* 316: 115–125, 2010.
16. De Mori R, Straino S, Di Carlo A, Mangoni A, Pompilio G, Palumbo R, Bianchi ME, Capogrossi MC, and Germani A. Multiple effects of high mobility group box protein 1 in skeletal muscle regeneration. *Arterioscler Thromb Vasc Biol* 27: 2377–2383, 2007.
17. Ellerman JE, Brown CK, de Vera M, Zeh HJ, Billiar T, Rubartelli A, and Lotze MT. Masquerader: high mobility group box-1 and cancer. *Clin Cancer Res* 13: 2836–2848, 2007.
18. Gardella S, Andrei C, Ferrera D, Lotti LV, Torrisi MR, Bianchi ME, and Rubartelli A. The nuclear protein HMGB1 is secreted by monocytes via a non-classical, vesicle-mediated secretory pathway. *EMBO Rep* 3: 995–1001, 2002.
19. Germani A, Limana F, and Capogrossi MC. Pivotal advances: high-mobility group box 1 protein—a cytokine with a role in cardiac repair. *J Leukoc Biol* 81: 41–45, 2007.
20. Grundtman C, Bruton J, Yamada T, Ostberg T, Pisetsky DS, Harris HE, Andersson U, Lundberg IE, and Westerblad H. Effects of HMGB1 on *in vitro* responses of isolated muscle fibers and functional aspects in skeletal muscles of idiopathic inflammatory myopathies. *FASEB J* 24: 570–578, 2010.
21. Hamanaka RB and Chandel NS. Mitochondrial reactive oxygen species regulate cellular signaling and dictate biological outcomes. *Trends Biochem Sci* 35: 505–513, 2010.
22. Hansen JM, Klass M, Harris C, and Csete M. A reducing redox environment promotes C2C12 myogenesis: implications for regeneration in aged muscle. *Cell Biol Int* 31: 546–553, 2007.
23. Harrison CA, Raftery MJ, Walsh J, Alewood P, Iismaa SE, Thliveris S, and Geczy CL. Oxidation regulates the inflammatory properties of the murine S100 protein S100A8. *J Biol Chem* 274: 8561–8569, 1999.
24. Jang YC, Lustgarten MS, Liu Y, Muller FL, Bhattacharya A, Liang H, Salmon AB, Brooks SV, Larkin L, Hayworth CR, Richardson A, and Van Remmen H. Increased superoxide *in vivo* accelerates age-associated muscle atrophy through mitochondrial dysfunction and neuromuscular junction degeneration. *FASEB J* 24: 1376–1390, 2010.
25. Ji LL. Antioxidant signaling in skeletal muscle: a brief review. *Exp Gerontol* 42: 582–593, 2007.
26. Kazama H, Ricci JE, Herndon JM, Hoppe G, Green DR, and Ferguson TA. Induction of immunological tolerance by apoptotic cells requires caspase-dependent oxidation of high-mobility group box-1 protein. *Immunity* 29: 21–32, 2008.
27. Kitahara T, Takeishi Y, Harada M, Niizeki T, Suzuki S, Sasaki T, Ishino M, Bilim O, Nakajima O, and Kubota I. High-mobility group box 1 restores cardiac function after myocardial infarction in transgenic mice. *Cardiovasc Res* 80: 40–46, 2008.
28. Kohno T, Anzai T, Naito K, Miyasho T, Okamoto M, Yokota H, Yamada S, Maekawa Y, Takahashi T, Yoshikawa T, Ishizaka A, and Ogawa S. Role of high-mobility group box 1 protein in post-infarction healing process and left ventricular remodelling. *Cardiovasc Res* 81: 565–573, 2009.
29. Leto TL, Morand S, Hurt D, and Ueyama T. Targeting and regulation of reactive oxygen species generation by Nox family NADPH oxidases. *Antioxid Redox Signal* 11: 2607–2619, 2009.
30. Livnat-Levanon N and Glickman MH. Ubiquitin-proteasome system and mitochondria—reciprocity. *Biochim Biophys Acta* 1809: 80–87, 2011.
31. Lotfi R, Herzog GI, DeMarco RA, Beer-Stolz D, Lee JJ, Rubartelli A, Schrezenmeier H, and Lotze MT. Eosinophils oxidize damage-associated molecular pattern molecules derived from stressed cells. *J Immunol* 183: 5023–5031, 2009.
32. Lotze MT, Zeh HJ, Rubartelli A, Sparvero LJ, Amoscato AA, Washburn NR, Devera ME, Liang X, Tor M, and Billiar T. The grateful dead: damage-associated molecular pattern molecules and reduction/oxidation regulate immunity. *Immunol Rev* 220: 60–81, 2007.
33. Manfredi AA, Capobianco A, Bianchi ME, and Rovere-Querini P. Regulation of dendritic- and T-cell fate by injury-associated endogenous signals. *Crit Rev Immunol* 29: 69–86, 2009.
34. Manfredi AA, Capobianco A, Esposito A, De Cobelli F, Canu T, Monno A, Raucci A, Sanvito F, Doglioni C, Nawroth PP, Bierhaus A, Bianchi ME, Rovere-Querini P, and Del Maschio A. Maturing dendritic cells depend on RAGE for *in vivo* homing to lymph nodes. *J Immunol* 180: 2270–2275, 2008.
35. McClung JM, Kavazis AN, Whidden MA, DeRuisseau KC, Falk DJ, Criswell DS, and Powers SK. Antioxidant administration attenuates mechanical ventilation-induced rat diaphragm muscle atrophy independent of protein kinase B (PKB Akt) signalling. *J Physiol* 585: 203–215, 2007.
36. Murton AJ, Constantin D, and Greenhaff PL. The involvement of the ubiquitin proteasome system in human skeletal muscle remodelling and atrophy. *Biochim Biophys Acta* 1782: 730–743, 2008.
37. Niethammer P, Grabher C, Look AT, and Mitchison TJ. A tissue-scale gradient of hydrogen peroxide mediates rapid wound detection in zebrafish. *Nature* 459: 996–999, 2009.
38. Oppenheim JJ and Yang D. Alarmins: chemotactic activators of immune responses. *Curr Opin Immunol* 17: 359–365, 2005.
39. Orlova VV, Choi EY, Xie C, Chavakis E, Bierhaus A, Ihanus E, Ballantyne CM, Gahmberg CG, Bianchi ME, Nawroth PP, and Chavakis T. A novel pathway of HMGB1-mediated inflammatory cell recruitment that requires Mac-1-integrin. *EMBO J* 26: 1129–1139, 2007.
40. Pallafacchina G, Francois S, Regnault B, Czarny B, Dive V, Cumano A, Montarras D, and Buckingham M. An adult tissue-specific stem cell in its niche: a gene profiling analysis of *in vivo* quiescent and activated muscle satellite cells. *Stem Cell Res* 4: 77–91, 2010.
41. Palumbo R, De Marchis F, Pusterla T, Conti A, Alessio M, and Bianchi ME. Src family kinases are necessary for cell migration induced by extracellular HMGB1. *J Leukoc Biol* 86: 617–623, 2009.
42. Palumbo R, Galvez BG, Pusterla T, De Marchis F, Cossu G, Marcu KB, and Bianchi ME. Cells migrating to sites of tissue damage in response to the danger signal HMGB1 require NF-kappaB activation. *J Cell Biol* 179: 33–40, 2007.

43. Powers SK, Duarte J, Kavazis AN, and Talbert EE. Reactive oxygen species are signalling molecules for skeletal muscle adaptation. *Exp Physiol* 95: 1–9, 2010.
44. Powis G and Kirkpatrick DL. Thioredoxin signaling as a target for cancer therapy. *Curr Opin Pharmacol* 7: 392–397, 2007.
45. Rando TA and Blau HM. Primary mouse myoblast purification, characterization, and transplantation for cell-mediated gene therapy. *J Cell Biol* 125: 1275–1287, 1994.
46. Rigoulet M, Yoboue ED, and Devin A. Mitochondrial ROS generation and its regulation mechanisms involved in H2O2 signaling. *Antioxid Redox Signal* 14: 459–468, 2011.
47. Rouhiainen A, Kuja-Panula J, Wilkman E, Pakkanen J, Stenfors J, Tuominen RK, Lepantalo M, Carpen O, Parkkinen J, and Rauvala H. Regulation of monocyte migration by amphoterin (HMGB1). *Blood* 104: 1174–1182, 2004.
48. Rubartelli A and Lotze MT. Inside, outside, upside down: damage-associated molecular-pattern molecules (DAMPs) and redox. *Trends Immunol* 28: 429–436, 2007.
49. Rubartelli A and Sitia R. Stress as an intercellular signal: the emergence of stress-associated molecular patterns (SAMP). *Antioxid Redox Signal* 11: 2621–2629, 2009.
50. Sampaolesi M, Torrente Y, Innocenzi A, Tonlorenzi R, D'Antona G, Pellegrino MA, Barresi R, Bresolin N, De Angelis MG, Campbell KP, Bottinelli R, and Cossu G. Cell therapy of alpha-sarcoglycan null dystrophic mice through intra-arterial delivery of mesoangioblasts. *Science* 301: 487–492, 2003.
51. Scaffidi P, Misteli T, and Bianchi ME. Release of chromatin protein HMGB1 by necrotic cells triggers inflammation. *Nature* 418: 191–195, 2002.
52. Scherz-Shouval R and Elazar Z. Regulation of autophagy by ROS: physiology and pathology. *Trends Biochem Sci* 36: 30–38, 2011.
53. Sciorati C, Touvier T, Buono R, Pessina P, Francois S, Perrotta C, Meneveri R, Clementi E, and Brunelli S. Necdin is expressed in cachectic skeletal muscle to protect fibers from tumor-induced wasting. *J Cell Sci* 122: 1119–1125, 2009.
54. Straino S, Di Carlo A, Mangoni A, De Mori R, Guerra L, Maurelli R, Panacchia L, Di Giacomo F, Palumbo R, Di Campli C, Uccioli L, Biglioli P, Bianchi ME, Capogrossi MC, and Germani A. High-mobility group box 1 protein in human and murine skin: involvement in wound healing. *J Invest Dermatol* 128: 1545–1553, 2008.
55. Tang D, Kang R, Cheh CW, Livesey KM, Liang X, Schapiro NE, Benschop R, Sparvero LJ, Amoscato AA, Tracey KJ, Zeh HJ, and Lotze MT. HMGB1 release and redox regulates autophagy and apoptosis in cancer cells. *Oncogene* 29: 5299–5310, 2010.
56. Tang D, Kang R, Livesey KM, Cheh CW, Farkas A, Loughran P, Hoppe G, Bianchi ME, Tracey KJ, Zeh HJ, 3rd, and Lotze MT. Endogenous HMGB1 regulates autophagy. *J Cell Biol* 190: 881–892, 2010.
57. Tang D, Kang R, Zeh HJ, and Lotze MT. HMGB1, oxidative stress, and disease. *Antioxid Redox Signal* 14: 1315–1335, 2011.
58. Tassi S, Carta S, Vene R, Delfino L, Ciriolo MR, and Rubartelli A. Pathogen-induced interleukin-1beta processing and secretion is regulated by a biphasic redox response. *J Immunol* 183: 1456–1462, 2009.
59. Tidball JG and Villalta SA. Regulatory interactions between muscle and the immune system during muscle regeneration. *Am J Physiol Regul Integr Comp Physiol* 298: R1173–R1187, 2010.
60. Urbonaviciute V, Furnrohr BG, Meister S, Munoz L, Heyder P, De Marchis F, Bianchi ME, Kirschning C, Wagner H, Manfredi AA, Kalden JR, Schett G, Rovere-Querini P, Herrmann M, and Voll RE. Induction of inflammatory and immune responses by HMGB1-nucleosome complexes: implications for the pathogenesis of SLE. *J Exp Med* 205: 3007–3018, 2008.
61. Urbonaviciute V, Meister S, Furnrohr BG, Frey B, Guckel E, Schett G, Herrmann M, and Voll RE. Oxidation of the alarmin high-mobility group box 1 protein (HMGB1) during apoptosis. *Autoimmunity* 42: 305–307, 2009.
62. Vene R, Delfino L, Castellani P, Balza E, Bertolotti M, Sitia R, and Rubartelli A. Redox remodeling allows and controls B cell activation and differentiation. *Antioxid Redox Signal* 13: 1145–1155, 2010.
63. Villeneuve NF, Lau A, and Zhang DD. Regulation of the Nrf2-Keap1 antioxidant response by the ubiquitin proteasome system: an insight into cullin-ring ubiquitin ligases. *Antioxid Redox Signal* 13: 1699–1712, 2010.
64. Wang H, Bloom O, Zhang M, Vishnubhakat JM, Ombrellino M, Che J, Frazier A, Yang H, Ivanova S, Borovikova L, Manogue KR, Faist E, Abraham E, Andersson J, Andersson U, Molina PE, Abumrad NN, Sama A, and Tracey KJ. HMG-1 as a late mediator of endotoxin lethality in mice. *Science* 285: 248–251, 1999.
65. Zedler S and Faist E. The impact of endogenous triggers on trauma-associated inflammation. *Curr Opin Crit Care* 12: 595–601, 2006.

Address correspondence to:
Dr. Patrizia Rovere-Querini
Innate Immunity and Tissue Remodeling Unit
San Raffaele Scientific Institute
Via Olgettina 58
Milano 20132
Italy

E-mail: rovere.patrizia@hsr.it

Date of first submission to ARS Central, May 30, 2010; date of final revised submission, January 17, 2011; date of acceptance, February 5, 2011.

Abbreviations Used

AEBSF = 4-(2-aminoethyl)benzenesulfonyl fluoride
BSA = bovine serum albumin
CTX = cardiotoxin
DAMPs = damage-associated molecular patterns
DMEM = Dulbecco's modified Eagle's medium
DTT = dithiothreitol
GM = growth medium
GSH = glutathione
H_2O_2 = hydrogen peroxide
HMGB1 = high-mobility group box 1
IGF = insulin-like growth factor 1
LC3 = light chain 3
NPSH = nonprotein thiols
PG1 = peroxy green
ROS = reactive oxygen species
SOD1 = superoxide dismutase 1
TA = tibialis anterior
Trx = thioredoxin

This article has been cited by:

1. Helena Erlandsson Harris, Ulf Andersson, David S. Pisetsky. 2012. HMGB1: A multifunctional alarmin driving autoimmune and inflammatory disease. *Nature Reviews Rheumatology* . [CrossRef]